EUROPEAN ORGANIZATION FOR NUCLEAR RESEARCH

CERN-EP/88-107
26.8.1988

XENON ISOTOPES FAR FROM STABILITY STUDIED BY COLLISIONAL IONIZATION LASER SPECTROSCOPY

W. BORCHERS, E. ARNOLD[1], W. NEU[1], R. NEUGART, K. WENDT
Institut für Physik, Universität Mainz, Fed.Rep.Germany
G. ULM[2]
and
The ISOLDE Collaboration
CERN, Geneva Switzerland

ABSTRACT

The new collisional reionisation scheme in collinear laser spectroscopy has enabled the study of hyperfine structures and isotope shifts of xenon isotopes over the large mass range A=116-146. The sensitivity of this method is demonstrated by the discovery of ^{146}Xe. Mean square charge radii, and spins and moments of the neutron-rich isotopes ^{137,139,141,143}Xe are deduced and discussed in comparison with earlier results on barium.

August 1988

(submitted to Phys. Lett. B)

(IS80)

[1] Present address: CERN, CH-1211 Geneva 23, Switzerland
[2] Present address: Physikalisch-technische Bundesanstalt, Institut Berlin, D-1000 Berlin 10.

Owing to laser-spectroscopic techniques, the information about nuclear spins, moments and radii in isotopic chains of the alkali and alkaline earth elements has become rather extensive. In the N = 82 region these elements include barium (Z = 56) [1] and caesium (Z = 55) [2] whose isotopes far from stability seem to develop well-deformed shapes. Therefore, it is of particular interest to study the transition into the near-spherical region of Z = 50. For Z = 54 the noble gas structure of xenon involves high electronic excitation energies which prevent laser spectroscopy in transitions from the $5p^6\ {}^1S_0$ ground state. However, the metastable J = 2 state of the configuration $5p^5 6s$ can serve as a basis, because it is efficiently populated in fast-beam charge transfer neutralization. Moreover, the particular features of the noble gas spectrum can be exploited for a new spectroscopic method of unprecedented sensitivity by optical pumping into the ground state and collisional ionization of the remaining metastable atoms. Here we report the first application of this technique [3] to the xenon isotopes far from stability.

The experiment was carried out at the ISOLDE mass separator at CERN. Neutron-deficient and neutron-rich isotopes are produced by the impact of 600 MeV protons on different targets. $^{116-130}$Xe are obtained from spallation in a molten-La target, and $^{136-146}$Xe from fission of uranium in the form of UC_2 heated to 2200°C. The products are guided to the plasma ion source through a cooled transfer line [4]. Natural xenon in the source is used to cover the intermediate range of stable isotopes.

The 60 keV Xe^+ beam is superimposed collinearly on the laser beam and then passes a caesium-vapour neutralization cell, where the metastable $5p^5 6s\ [3/2]_2$ atomic state is populated by near-resonant

charge transfer. The laser excitation to $5p^5 6p\ [3/2]_2$ is detected either by fluorescence or by the new scheme of collisional ionization and ion counting (Fig. 1). For this purpose a differentially pumped gas target is installed downstream from the optical excitation region, and the ions created here are deflected onto the cathode of a secondary electron multiplier.

This scheme utilizes the large cross-section for electron stripping from atoms in the high-lying metastable $5p^5 6s\ [3/2]_2$ state. The relevant part of the energy level diagram of xenon is shown in Fig. 2. Laser excitation to $5p^5 6p\ [3/2]_2$ at 823 nm depopulates the metastable level and pumps the atoms into the $5p^6\ {}^1S_0$ ground state. Thus the resonance is detected via the optical pumping process as a drop-out in the ion counting.

Considering the sensitivity we find for ^{146}Xe with 400 atoms/s from ISOLDE that a clear signal (S/N = 5) is recorded within 35 min. This has to be compared to the limit of standard fluorescence detection which for xenon amounts to about 10^6 atoms/s. The huge gain is ascribed to two reasons: (i) inefficient photon detection is replaced by very efficient ion detection; (ii) the dominant stray-light background of fluorescence measurements is totally eliminated. These features have been exploited similarly for spectroscopy on the alkaline earth ions, where optical pumping is detected by a change in the charge transfer neutralization rate [5]. On the other hand, the particle detection has to cope with sources of background that are different in nature: (i) Isobaric beam contamination from reaction products or impurities in the target or ion source can easily exceed the xenon yields by several orders of magnitude. Such a contamination is largely avoided by careful outgassing and by

trapping of the less volatile products and impurities from the target in the water-cooled transfer line to the ion source. (ii) The ion detector is also sensitive to radioactivity collected during the measurements. Therefore, the cathode consists of an aluminized mylar tape which can be moved by remote control. Still, a typical rate of 10-20 counts/s arises from background radioactivity.

Apart from this background the sensitivity is mainly determined by the efficiency and state selectivity of the ionization process. The total ionization efficiency as a function of the target gas pressure is limited by reneutralization, and the flop-out signal for complete optical pumping depends on the non-vanishing cross-section for ionization from the ground state. The best compromise between ionization efficiency and selectivity was obtained with a $10^{15}/cm^2$ Cl_2 target. A quantitative estimate of the sensitivity limit can be based on the following numbers: 50 % total transmission of the beam line and the apparatus, 50 % neutralization and 10 % reionization efficiency with a 50 % flop-out signal on the ion current. This shows that signals from less than 100 atoms/s can be detected within reasonable measuring time. Improvements may be expected from a more detailed investigation of the fast-atom collision processes.

The spectra of $^{116-118}Xe$ and $^{141-146}Xe$ were obtained by recording the ion count rate versus the acceleration voltage (Doppler tuning). As an example Fig. 3 shows the ^{141}Xe hyperfine structure (hfs) pattern which corresponds to a magnetic moment close to zero and a large quadrupole moment. For the remaining isotopes $^{120-142}Xe$ the yields are sufficient for optical detection. As a reference for isotope shift (IS) evaluations the spectrum of a stable isotope (^{136}Xe or ^{130}Xe) was periodically recorded during all measurements.

Changes in the nuclear mean square charge radii relative to ^{136}Xe were deduced from the IS data (Table 1). The evaluation is analogous to that described in ref. [6]. In the extraction of field shifts from the observed IS the specific mass shift (SMS) was estimated to be zero with an error of ± the normal mass shift (NMS). This is suggested by the opposite sign of estimates by King [7] and earlier authors and results from recent muonic data [8]. The value for the electron density at the site of the nucleus was derived from the $5p^5ns$ level energies, for which the Goudsmit-Fermi-Segrè formula yields $|\psi_{6s}(0)|^2 = 2.85\ a_0^{-3}$. We used the screening factor $\beta = 1.16$ [7] and the IS constant $C_{unit} = 44.37$ mK [9].

The new $\delta\langle r^2\rangle$ values for xenon may be compared with the corresponding results for the neighbouring even-Z element barium. In Fig. 4 both $\delta\langle r^2\rangle$ chains are plotted against the neutron number N. As a dominant feature they show the distinct kink at the neutron shell closure N = 82 which is conventionally explained by increasing dynamic and static deformation on either side. This qualitative interpretation is supported by the trend of a less pronounced kink for xenon (Z = 54), corresponding to the neighbourhood of the magic proton number Z = 50. For the neutron-deficient isotopes the xenon data beyond midshell (N = 66) suggest a parabolic trend similar to the one pointed out first for the cadmium isotopes between N = 54 and 72 [13]. However, a fit to the data shows that this picture already has to be modified four protons away from the shell closure: From N = 82 to N = 68 the radii develop almost linearly, and around midshell the increasing deformation saturates at an equilibrium value of $\beta_2 \approx 0.3$ which is roughly consistent with the information from B(E2) values [14].

From the hfs of the odd neutron-rich isotopes were determined the nuclear spins as well as the magnetic and electric hyperfine parameters A and B (Table 2). The magnetic moments were evaluated using as reference values the magnetic moment [15] and the precise hfs constant for the metastable state [16] of ^{129}Xe. The errors of μ were chosen as to account for hfs anomaly effects which would be reflected in the A-factor ratio between the metastable $5p^5 6s$ and the excited $5p^5 6p$ state. The spectroscopic quadrupole moments were obtained taking as reference Q_s = -0.116(4) b from a recent measurement of the hfs in muonic ^{131}Xe [17]. This essentially confirms the semi-empirical analysis of the optical hfs by Faust and McDermott [16], indicating a small Sternheimer shielding correction.

In the presently investigated series of odd-A nuclei, $^{137-143}$Xe, the spins follow exactly those of the isotones $^{139-145}$Ba [1]. This similarity suggests a direct comparison of the individual moments which for barium were interpreted [1] within the particle-rotor scheme. The neutron orbitals above N = 82 originate from the $f_{7/2}$, $h_{9/2}$ and $i_{13/2}$ shell model states. For N = 83 and N = 85 the isotones in barium and xenon have rather similar moments, and the interpretation of ^{137}Xe as a spherical $f_{7/2}$ state and ^{139}Xe as a 3/2$^-$ state with the main component from [532 3/2] can be directly inferred from the arguments given for ^{139}Ba and ^{141}Ba. A decoupled configuration is suggested for N = 87 by the negative quadrupole moments of ^{143}Ba and ^{141}Xe. The very small magnetic moment of ^{141}Xe can be explained by a similar 5/2$^-$ level as in ^{143}Ba, built on the main components from [530 1/2] and [532 3/2]. An interesting case is N = 89 where Leander et al. [18] state the influence of octupole deformation on the single-particle structure around ^{145}Ba. The

reflection-asymmetric potential gives rise to a substantial lowering of the [523 5/2] level towards the Fermi energy at A = 145. It is surprising to find this level again as the ground state of ^{143}Xe. One has to conclude that reflection-asymmetric orbitals persist for the N = 89 nuclei even close to Z = 50. The magnetic moment which is rather insensitive to β_3 [18] becomes smaller for xenon, as it is expected for smaller quadrupole deformation β_2 [19].

Measurements on the neutron-deficient odd-A isotopes are in progress. Obvious extensions of the technique can be found in studies of the radon isotopes at the borderline of the octupole deformed region of Ra-Th nuclei around A = 224, and the krypton isotopes around N = 38 and N = 60.

This work has been funded by the German Federal Minister for Research and Technology (BMFT) under the contract number 06 MZ 458 I.

References

[1] A.C. Mueller et al., Nucl. Phys. A 403 (1983) 234

[2] C. Thibault et al., Nucl. Phys. A 367 (1981) 1

[3] R. Neugart, W. Klempt and K. Wendt, Nucl. Instr. Meth. B 17 (1986) 354

[4] T. Bjørnstad et al., Physica Scripta 34 (1986) 578

[5] R.E. Silverans, P. Lievens and L. Vermeeren, Nucl. Instr. Meth. B 26 (1987) 591;
R.E. Silverans et al., Phys. Rev. Lett. 60 (1988) 2607

[6] S.A. Ahmad et al., Nucl. Phys. A 483 (1988) 244

[7] W.H. King, Isotope Shifts in Atomic Spectra, Plenum Press (New York 1984)

[8] Th. Hennemann and G. Fricke, private communication

[9] S.A. Blundell et al., Z. Phys. A 321 (1985) 31

[10] W.D. Myers and K.-H. Schmidt, Nucl. Phys. A 410 (1983) 61;
D. Berdichevsky and F. Tondeur, Z. Phys. A 322 (1985) 141

[11] D.A. Eastham et al., Proc. 5th Int. Conf. on Nuclei Far from Stability, ed. I.S. Towner (AIP Conf. Proc. 164) p. 136

[12] K. Wendt et al., Z. Phys. A 329 (1988) 407

[13] F. Buchinger et al., Nucl. Phys. A 462 (1987) 305

[14] S. Raman et al., At. Data Nucl. Data Tables 36 (1987) 1

[15] C.M. Lederer and V.S. Shirley, Table of Isotopes, 7th ed. (Wiley, New York, 1978)

[16] W.L. Faust and M.N. McDermott, Phys. Rev. 123 (1961) 198

[17] Th. Hennemann, Thesis KPH 9/88 (Mainz, 1988)

[18] G.A. Leander et al., Phys. Lett. 152 B (1985) 284

[19] C. Ekström and I.-L. Lamm, Physica Scripta 7 (1973) 31

FIGURE CAPTIONS

Figure 1: Schematic view of the experimental setup.

Figure 2: Level structure of Xe. The 6s $[3/2]_2$ level is populated by charge transfer from the Cs ground state. The pumping process is indicated by arrows.

Figure 3: Hyperfine structure of ^{141}Xe recorded by the particle detector.

Figure 4: Development of the charge radii in Xe (Z = 54) and Ba (Z = 56) with droplet model [10] isodeformation lines. Recent results for ^{120,121}Ba [11] and ^{148}Ba [12] have been added to the Ba curve of ref. [1]. Preliminary data are included for the light odd-A Xe isotopes.

Table 1: Isotope shift and deduced $\delta\langle r^2\rangle$ relative to ^{136}Xe. Round brackets indicate experimental errors, while square brackets give the errors due to uncertainties in the SMS and the electronic Factor F.

A	IS (MHz)	$\delta\langle r^2\rangle^{136,A}$ (fm^2)
116	1120 (19)	-0.599 (9) [140]
118	833 (17)	-0.460 (7) [120]
120	643 (16)	-0.363 (7) [110]
122	523 (13)	-0.299 (6) [90]
124	418 (11)	-0.242 (5) [80]
126	330 (16)	-0.193 (7) [60]
128	261 (10)	-0.152 (4) [50]
129	271 (7)	-0.152 (3) [40]
130	203 (6)	-0.117 (3) [40]
131	229 (6)	-0.124 (2) [30]
132	150 (4)	-0.0844 (17) [200]
134	97 (3)	-0.0518 (13) [120]
136	0	0
137	-224 (6)	0.105 (3) [10]
138	-545 (6)	0.254 (3) [20]
139	-769 (13)	0.359 (6) [30]
140	-1042 (5)	0.486 (2) [40]
141	-1266 (9)	0.591 (4) [50]
142	-1522 (20)	0.710 (9) [60]
143	-1698 (8)	0.794 (4) [70]
144	-1943 (10)	0.908 (5) [80]
146	-2352 (12)	1.100 (5) [100]

Table 2: Nuclear spins, hyperfine parameters A_m, B_m for the metastable $5p^5 6s\ [3/2]_2$ state and A_e, B_e for the excited $5p^5 6p\ [3/2]_2$ state, and deduced nuclear magnetic dipole moments μ and electric quadrupole moments Q_e.

A	I	A_m (MHz)	A_e (MHz)	μ (n.m.)	B_m (MHz)	B_e (MHz)	Q_e (b)
129	1/2	-2384.5031(4)[a]	-886.1(8)	-0.777976(9)[b]			
131	3/2	706.47422(18)[a]	263.1(6	0.691861(4)[b]	252.5263(6)[a]	29(2)	-0.116(4)[c]
137	7/2	-424 (2)	-157 (1)	-0.968(8)	1050(16)	126(9)	-0.48(2)
139	3/2	-311 (6)	-115 (3)	-0.304(10)	-865(18)	-107(10)	0.40(2)
141	5/2	6.3(9)	2.1(7)	0.010(4)	1259(7)	150(6)	-0.58(2)
143	5/2	-281.9(3)	-104.9(3)	-0.4599(14)	-2025(3)	-244(3)	0.93(3)

[a] from ref. [16]
[b] from ref. [15]
[c] from ref. [17]

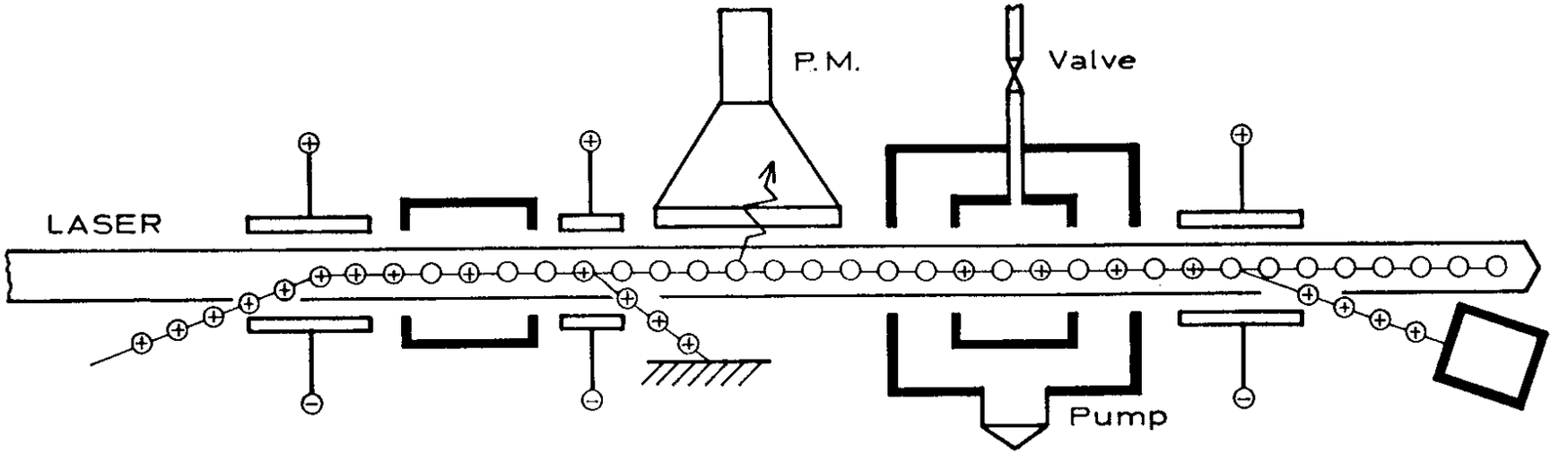
P.M.
Valve
LASER
Pump
Charge Exchange
Optical Detection
Gas Target
Particle Detection

figure 1

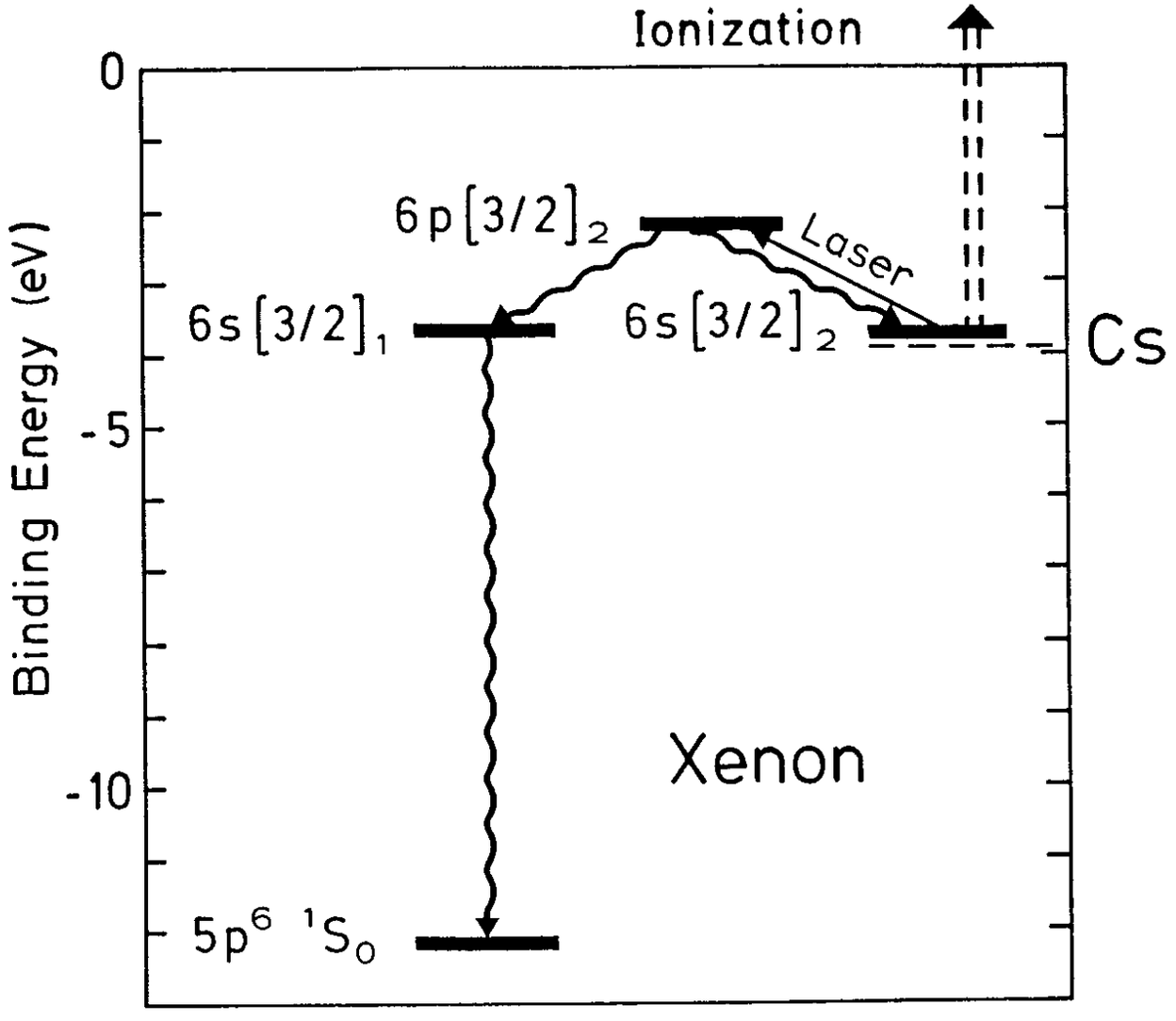
Ionization
0
-5
-10
Binding Energy (eV)
6p[3/2]2
Laser
6s[3/2]1
6s[3/2]2
Cs
Xenon
5p6 1S0

figure 2

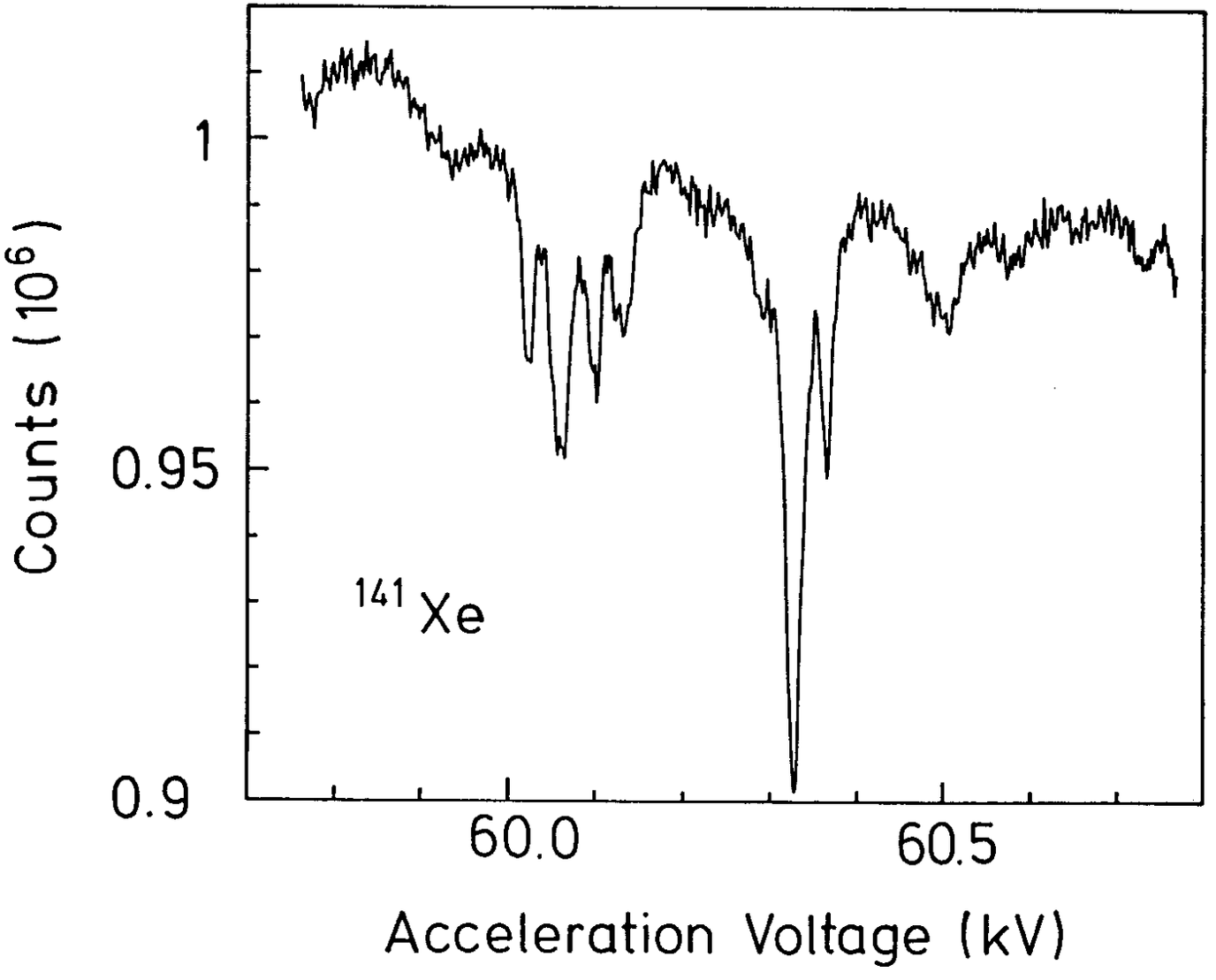

figure 3

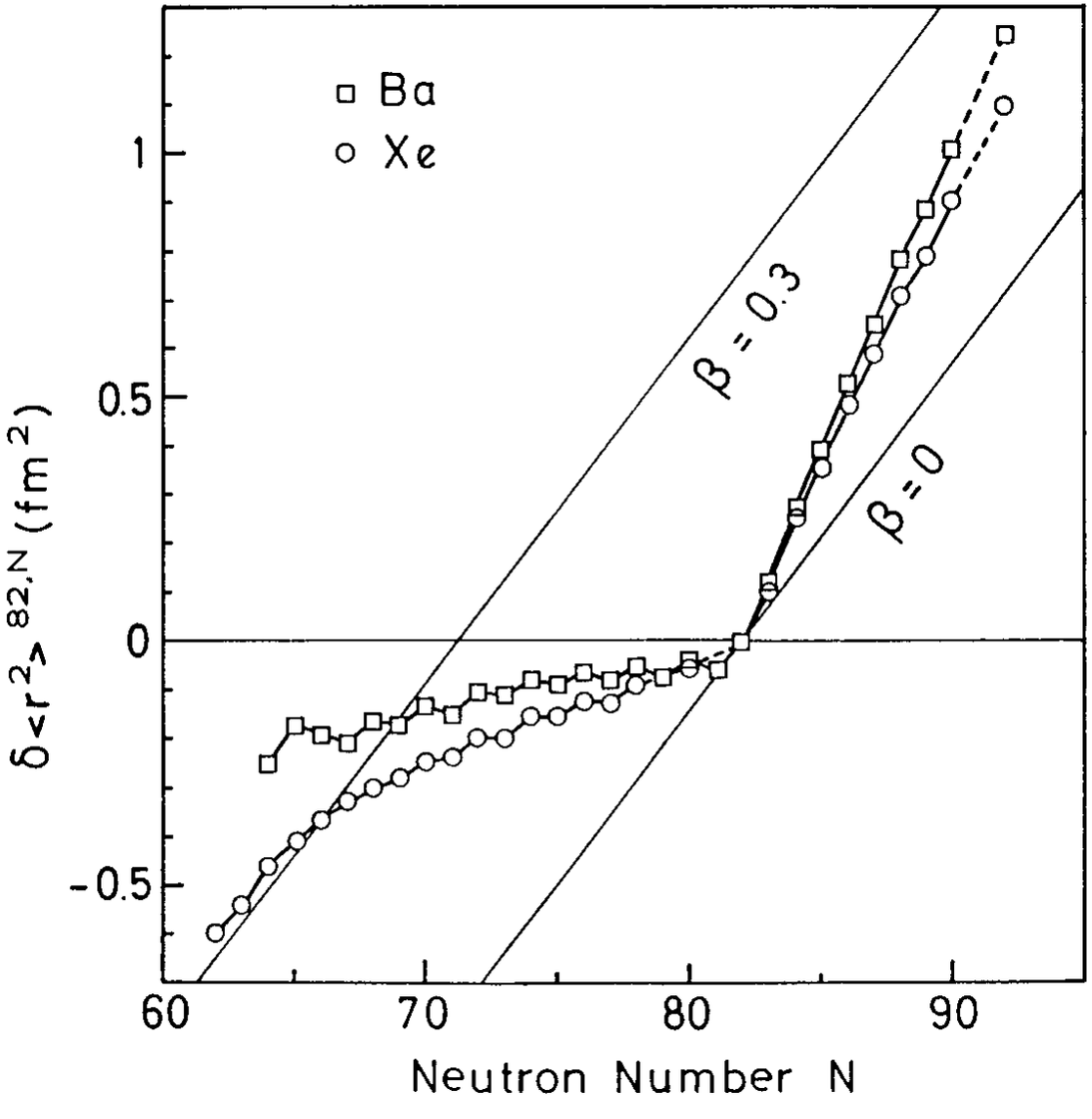

figure 4